RSC Advances

ROYAL SOCIETY OF CHEMISTRY

www.rsc.org/advances

Journal Name

ARTICLE

Fe_3O_4-decorated single-walled carbon nanohorns with extraordinary microwave absorption property

Received 00th January 20xx,
Accepted 00th January 20xx

DOI: 10.1039/x0xx00000x

www.rsc.org/

Longbin Cui[a,b], Yang Liu[b], Xiaohui Wu[b], Ziqi Hu[b], Zujin Shi[b*] and Huanjun Li[a*]

Single-walled carbon nanohorns (SWCNHs) is seldom used as electromagnetic (EM) wave absorption material due to its inferior impedance matching resulting from its high dielectric constant. In this work, decorated with 35.6wt.% Fe_3O_4 nanoparticles, the as-prepared composite displays a significantly enhanced EM wave absorption ability because of the improved impedance matching, electric polarization and interfacial polarization. Specifically, the maximum reflection loss of this composite with a thickness of 5.8mm is -38.84dB at 3.72GHz in S-band. The bandwidth of absorption exceeding -10dB is 9.2GHz (from 3.2GHz to 12.4GHz) with the absorber thickness of 2-6mm. What is more, a second absorption peak with the reflection loss no less than -10dB appears when the absorber thickness is over 4mm.

Introduction

Electromagnetic (EM) pollution is a growing problem around us due to popular application of EM techniques. It endangers public health and safety enormously[1]. Therefore, studying of the EM absorption materials has attracted extensive attention. Recently, carbon nanomaterials, particularly CNTs and graphene, have been widely investigated as potential wave absorbing materials[2]. The high dielectric constant, the low density, the large surface area[3] and excellent thermal stability[4] make them extraordinarily eligible for EM wave absorption materials. However, the EM wave absorption abilities are far from satisfaction because of poor impedance matchings when they used alone[5]. To address this issue, a series of novel composites are prepared via loading metal or metaloxide nanoparticles on a nanostructured carbon matrix, like Fe_3O_4/MWCNTs[4], r-GO/Fe_3O_4[5b], Fe/MWCNT[6], Ni/graphene[7] and Ag/CNT[8]. In contrast to the pure carbon nanomaterials, these composites have an improved impendence matching as a result of their reduced dielectric constant.

Single-walled carbon nanohorns (SWCNHs), a new carbon nanomaterial found during producing SWCNTs[9], has been widely studied in different fields recently, such as gas storage, adsorption, catalyst support and drug delivery[10]. However, there is no research about wave absorption of SWCNHs. SWCNHs has the aforementioned merits like other carbon nanomaterials[11]. Compared with the production process of CNTs, there is no need of expensive metal catalysts for preparation of SWCNTs, which facilitates the low-cost and large-scale industrial production in the future. Consequently, SWCNHs will be more promising as EM wave absorption material. Nevertheless, SWCNHs also suffers from the poor impendence matching due to its high dielectric constant. Therefore, improvement of such property is indispensable.

Fe_3O_4, a typical magnetic loss material for EM wave absorption, has abundant sources and has been extensively studied[12]. It is a reasonable program to combine SWCNHs with Fe_3O_4 NPs to form binary composites as better EM wave absorption materials. To our best acknowledge, however, Fe_3O_4/SWCNHs composite has been rarely researched and its EM wave absorption property has not been reported yet.

In this work, Fe_3O_4/SWCNHs composite is synthesized with a facile method and its EM wave absorption property is studied. Its amazing EM wave absorption ability may make it be applied to the stealth technology or EM compatibility technology.

Experimental

Preparation of SWCNHs dispersion

SWCNHs was produced using an arc-discharge method as described in our previous report[12] and oxidated by a mixture of concentrated acid (the volume ratio of H_2SO_4/HNO_3 is 3:1) to improve its chemical activity and dispersibility in aqueous solution. 200mg oxidated SWCNHs (ox-SWCNHs) were ultrasonically dispersed in 800mL deionized water for 60min and then divided into four portions equally.

Preparation of Fe_3O_4/SWCNHs composites and Fe_3O_4 nanoparticles[13]

Fe_3O_4/SWCNHs composites were prepared with a facile two-step synthetic method. Briefly, 1.0g iron(III) acetylacetonate was dissolved in 150mL triethylene glycol (TREG), and then heated to 278°C slowly and kept at reflux for 30min under the

[a] Department of Applied Chemistry & Pharmaceutical, School of Chemical Engineering and Environment, Beijing Institute of Technology, Beijing 10081, P.R. China. E-mail: lihj@bit.edu.cn; Tel: +86 1068915830
[b] Beijing National Laboratory for Molecular Sciences, State Key Lab of Rare Earth Materials Chemistry and Applications, College of Chemistry and Molecular Engineering, Peking University, Beijing 100871, P.R. China. E-mail: zjshi@pku.edu.cn; Tel: +86 1062751495
DOI: 10.1039/x0xx00000x

protection of nitrogen. After cooling down, 5, 15, 30 and 60mL Fe_3O_4 TREG dispersion were added into the three prepared ox-SWCNHs dispersion respectively. The resultant mixture were stirred over night at room temperature. Then the suspensions were centrifuged and the precipitate were alternately washed 3 times with ethanol and deionized water. Lastly, Fe_3O_4/SWCNHs composites were obtained after being dried in a vacuum oven at 60°C for 12h. The three samples were named as S1, S2, S3 and S4.

The Fe_3O_4 nanoparticles (NPs) were separated by a magnet from the Fe_3O_4 TREG dispersion that was diluted by moderate dosage of ethanol in advance, then washed by ethanol and deionized water and subsequently dried in a vacuum oven at 60°C for 12h.

Characterization

The morphologies of samples were characterized by a transmission electron microscopy (TEM, Hitachi H9000NAR) .The X-ray diffraction (XRD) patterns were recorded on a Rigaku D/max-2000 using filtered Cu Kα radiation. Fourier transform infrared (FTIR) spectra of samples in the range of 400-4000cm^{-1} were investigated with an infrared spectrometric analyzer (VECTOR 22) using the KBr pellet method. The chemical states of elements were investigated by X-ray photoelectron spectroscopy (XPS, Axis Ultra). Superconducting quantum interference device (SQUID, Quantum Design MPMS-XL5) was used to study the magnetic properties of composites at room temperature. The electromagnetic parameters were measured on a vector network analyzer (HP-8722ES) in the frequency range of 2–18 GHz. In advance, the samples were prepared by uniformly mixing the composites with 50wt.% epoxy and pressing into a cylindrical shape with Φ_{out} of 7.00 mm, Φ_{in} of 3.00 mm, and thickness of 2.00 mm. The weight ratio of SWCNHs to Fe_3O_4 was determined by the residual weight after the composites was treated by concentrated hydrochloric acid for 6h and the results are listed in Table 1.

Table. 1. The weight ratio of Fe_3O_4 of S1, S2, S3 and S4

Sample	M_0[a] / mg	M_1[b] / mg	Wt.[c] %
S1	50.1	38.3	23.55
S2	50.0	32.2	35.60
S3	50.3	22.7	54.87
S4	50.4	17.2	65.87

[a] M_0 is the mass of sample before the treatment with concentrated hydrochloric acid. [b] M_1 is the weight of residuum treated by acid. [c] Wt.% is the weight ratio of Fe_3O_4 in the composite.

Results and discussion

Morphology and structure

The TEM images of the ox-SWCNHs, Fe_3O_4 NPs and Fe_3O_4/SWCNHs hybrid materials are shown in Fig 1. At low magnification (Fig. 1a), the ox-SWCNHs emerge as spherical aggregates with diameters of 100-150nm. At high magnification (Fig. 1a inset), the defect in the conic node of the SWCNHs after oxidation was observed and indicted by red circle. These defects will create localized states near to Fermi level, which facilitates EM energy absorption by electron transition from contiguous states to Fermi level when the EM wave is radiated on the absorber surface[5a, 5b]. The Fe_3O_4 NPs are uniform in diameters from 8nm to 10nm (Fig. 1b), which is in the size range of superparamagnetism. Fig. 1c, d, e and f reveal that Fe_3O_4 NPs have successfully loaded on the SWCNHs. With the increase of the input of Fe_3O_4, the loading amount of Fe_3O_4 becomes larger.

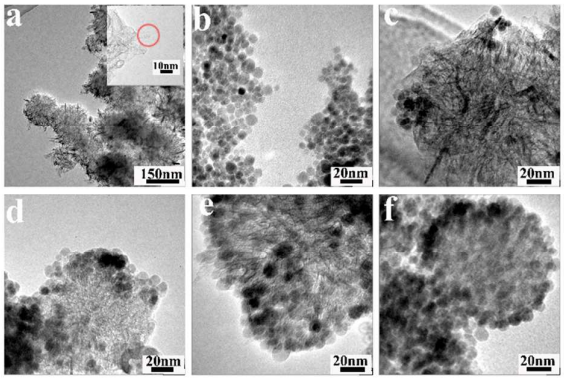

Fig.1. TEM images of ox-SWCNHs(a), Fe_3O_4 NPs(b), S1(c), S2(d), S3(e) and S4(f). The inset of (a) is the magnified picture of ox-SWCNHs with defects indicted by red circle.

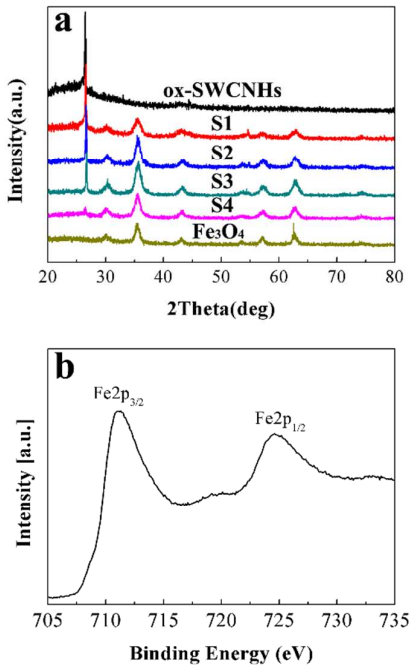

Fig.2. (a) XRD patterns of Fe_3O_4, ox-SWCNHs, S1, S2, S3 and S4; (b) The Fe2p core level XPS spectrum.

Meanwhile, it is beneficial to absorb EM wave that the nanoparticles on the SWCNHs are not aggregated.

In order to obtain the structure information of the composites, XRD characterization was conducted. Fig.2a shows the XRD patterns of ox-SWCHNs, Fe_3O_4 and Fe_3O_4/SWCNHs composites. It is obvious that the peaks (2θ=30.4, 35.6, 43.3, 53.4, 57.3, and 62.8°) of all composites correspond to the diffractions of (220), (311), (400), (422), (511) and (400) planes of Fe_3O_4, respectively. And the peak at 2θ=26.4° is assigned to the diffraction of (002) plane of SWCNHs. The peak intensity of SWCNHs weakens with the increasment of Fe_3O_4 content, while those of Fe_3O_4 become stronger. Moreover, the XRD

diffraction patterns of composites also confirm that Fe_3O_4 has loaded on the SWCNHs successfully. Besides, the average size of Fe_3O_4 NPs calculated using Scherrer Equation is 8.7nm, which agree well with the results observed by TEM. Because the X-ray diffraction peaks of γ-Fe_2O_3 are extremely similar to those of Fe_3O_4, XPS measurement is necessary to ensure the valence states of Fe element. In Fig.2b, the binding energies of Fe2p appear at 711.1eV and 724.6eV and there is no satellite peak at 720eV. It demonstrates that the composition of nanoparticles is Fe_3O_4.

Fig.3 represents a comparison of the FT-IR spectra of ox-SWCNHs, Fe_3O_4 NPs, and S2. The peaks of ox-SWCNHs are ascribed to stretching modes of O-H (υ_{O-H}=3427cm^{-1}), C=O ($\upsilon_{C=O}$=1728cm^{-1}), C=C ($\upsilon_{C=C}$=1577cm^{-1}) and C-O-C (υ_{C-O} at 1157 and 1030cm^{-1}) bonds. The absorption of Fe_3O_4 at 588cm^{-1} is attributed to stretching vibration of Fe-O. Compared with that of ox-SWCNHs, the peak of υ_{Fe-O} in the spectrogram of S1 further verifies the existence of Fe_3O_4 NPs in the composites. The disappearance of peak of υ_{O-H} suggests Fe_3O_4 NPs are actively interacting with SWCNHs by bidentate coordination of Fe element with carboxylate group and replacement of hydrogen in hydroxyl groups[14].

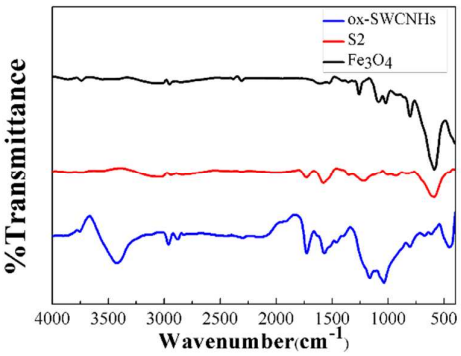

Fig.3. The FT-IR spectra of ox-SWCNHs, Fe_3O_4 NPs and S2.

Magnetic property

The magnetic properties of the composites and as-produced Fe_3O_4 NPs were examined at 300K on a superconducting quantum interference device and are shown in Fig. 4. Obviously, the coercivity of Fe_3O_4 NPs is zero, which indicates the nanoparticles are superparamagnetic. The saturation magnetization values of three composite samples are 16.53, 25.23, 37.47 and 41.34 emu·g^{-1} respectively, while that of Fe_3O_4 NPs is 64.74 emu·g^{-1}. Notably, that the saturation magnetization is greater with a higher ratio of Fe_3O_4 content.

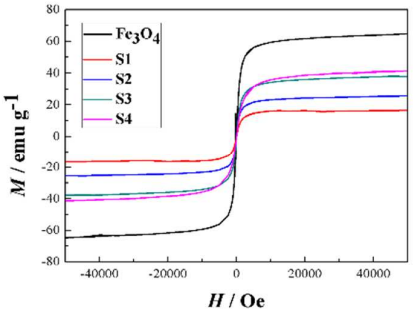

Fig.4.The magnetization hysteresis loops of the as-prepared Fe_3O_4 NPs and composites measured at room temperature.

Microwave absorption property

The reflection losses of ox-SWCNHs, Fe_3O_4 NPs and each composite are measured in the frequency range of 2–18 GHz. Microwave absorption property is evaluated by the reflection loss (RL) calculated with the following equations:

$$Z_{in} = \sqrt{\mu_r/\varepsilon_r}\ \tanh[j(2\pi fd/c)\sqrt{\mu_r\varepsilon_r}] \quad (1)$$

$$R_L(dB) = 20\log|(Z_{in}-1)/(Z_{in}+1)| \quad (2)$$

Where the μ_r and ε_r are the relative complex permeability and permittivity respectively, f is the frequency of the electromagnetic waves, d is the thickness of absorber, c is the velocity of electromagnetic waves in free space. The reflection losses of each measured sample with a thickness range from 2 to 6mm are showed in Fig.5. ox-SWCNHs displays an unsatisfactory EM wave absorption property with the maximum RL being below –10dB (Fig.5a). After being decorated with Fe_3O_4 NPs, the values of reflection losses change dramatically (Fig.5b, e, c and d). Overall the values rise firstly and then run down with the increasing weight ratio of Fe_3O_4. Obviously, S2 exhibits the best EM wave absorption ability. To be specific, the bandwidth of S2 is 9.2GHz (from 3.2GHz to 12.4GHz), in which the RL is greater than -10dB for the absorber. When the thickness is 5.8mm, RL reaches the maximum value (-38.84dB) at 3.72GHz which is in S-band. The EM wave absorption materials[5c, 5d, 6, 7] reported with exceptional EM wave absorption property in S-band are not common. Moreover, when the absorber thickness reaches 4mm, a second absorption peak appears and the RL of this peak can reach -10dB. Although the maximum loss of S3(-38.75dB) is approximate to that of S2, It is worth noting that its bandwidth is 5.1GHz (from 12.9GHz to 18GHz) and is much narrower than that of S2. In addition, the as-prepared Fe_3O_4 NPs show a relatively weak EM wave absorption (Fig.5f).

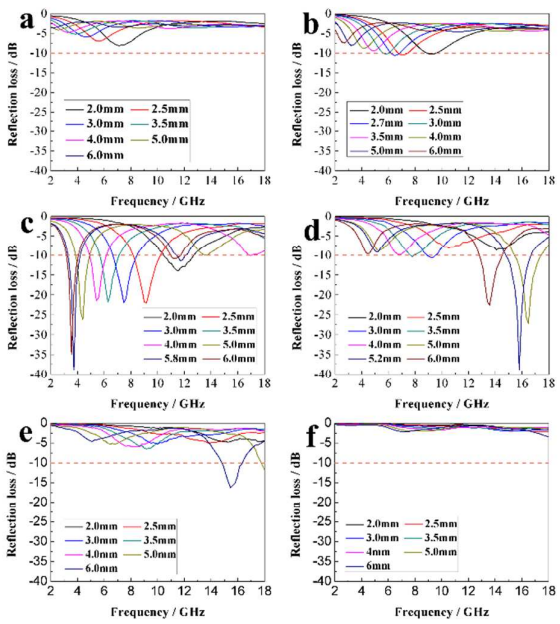

Fig. 5. The reflection loss of (a)ox-SWCNHs, (b)S1, (c)S2, (d)S3 (e)S4 and (f)Fe_3O_4 with a thicknesses range from 2 to 6 mm.

Electromagnetic parameter analysis

It is well known that the complex permeability ($\mu_r=\mu'-j\mu''$) and permittivity ($\varepsilon_r=\varepsilon'-j\varepsilon''$) play an important role in EM wave absorption. The real part of complex permittivity ε' and the imaginary part ε'' are shown in Fig 6a and 6b. ox-SWCNHs, a typical dielectric loss material for microwave absorption has the highest ε' and ε'' compared with other measured samples. On the contrary, Fe_3O_4 presents the lowest ε' and ε''. When ox-SWCNHs are loaded with Fe_3O_4 NPs, both ε' and ε'' run down and become nearly constant. The larger weight ratio of Fe_3O_4 is, the smaller values of ε' and ε'' are exhibited. In Fig 6c and 6d, it displays the complex permeability real part μ' and imaginary part μ''. The μ' values of each sample rise slightly with the rise of Fe_3O_4 content. The μ'' values of each measured samples are less than 0.3 over 2-18GHz. The low μ'' values indicate dielectric loss may be the main factor determining the EM wave absorbing performances of composites.

For further studying the EM absorbing mechanism of the composites, the dielectric loss factor ($\tan\delta_E=\varepsilon''/\varepsilon'$) and magnetic loss factor ($\tan\delta_M=\mu''/\mu'$) were calculated and shown in Fig.7. The $\tan\delta_M$ of measured samples are low and similar with each other. In compared to ox-SWCNHs and S1, S2 has a lower $\tan\delta_E$ but much closer values of $\tan\delta_E$ and $\tan\delta_M$ in the frequency range of 2-18GHz. It demonstrates that S2 has an improved impedance matching, which may explain why S2 has better EM wave absorbing property than ox-SWCNH and S1 do. When the weight ratio of Fe_3O_4 is elevated, $\tan\delta_E$ and $\tan\delta_M$ become much closer, but the $\tan\delta_E$ drops substantially, which leads to a low consumption when the EM energy penetrates the absorber. Therefore, S2 is better as EM wave absorber than S3 and S4, although the latter ones possess more appropriate impedance matching. In addition, despite that the as-prepared Fe_3O_4 NPs also have a suitable fine impedance matching, they suffer from relatively low $\tan\delta_E$ and $\tan\delta_M$, which results in weak EM wave absorption.

After being loaded with Fe_3O_4 NPs, the composite gains reduced dielectric constants relative to those of bare ox-SWCNHs. And hence an improved impedance matching is achieved. In the meantime, an interfacial polarization between the two phases of Fe_3O_4 and ox-SWCNHs can lead to an additional dielectric loss. Furthermore, there is also an electronic transference between Fe^{2+} and Fe^{3+} ions that can generate charge polarization. All above characteristics ultimately enable S2 to represent more outstanding wave absorption capability.

Journal Name

ARTICLE

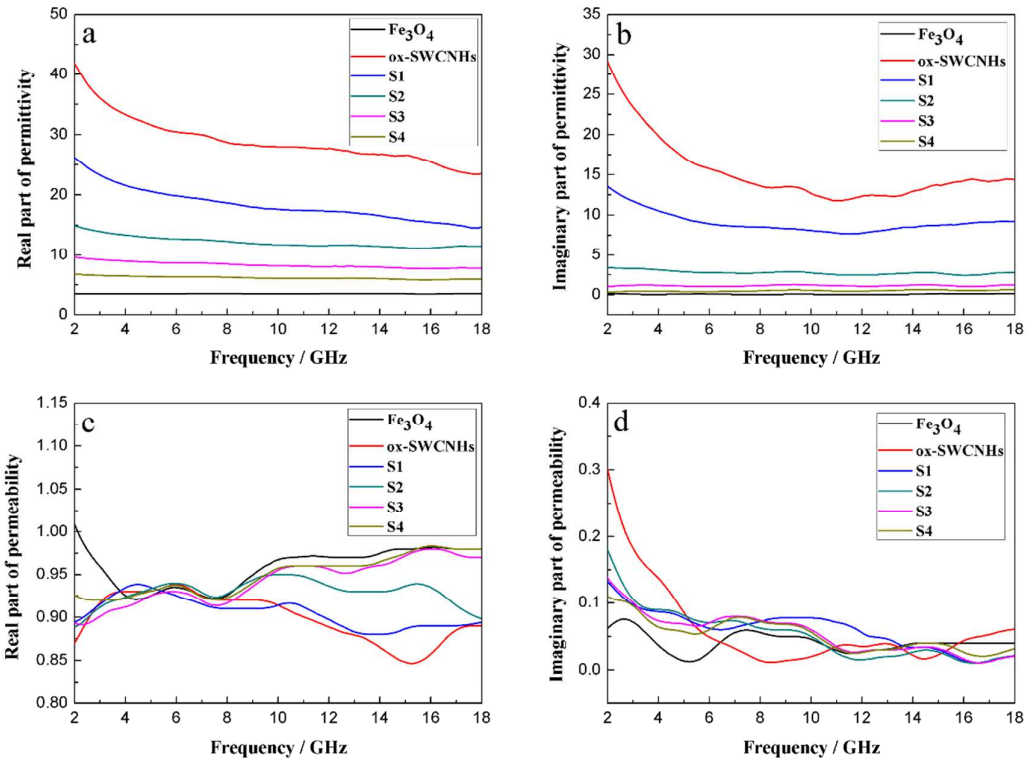

Fig.6. Permittivity and permeability characterizations of the six samples in the 2 −18 GHz range: (a) real part of complex permittivity spectra, (b) imaginary part of complex permittivity spectra, (c) real part of complex permeability spectra and (d) imaginary part of complex permeability spectra.

Journal Name

ARTICLE

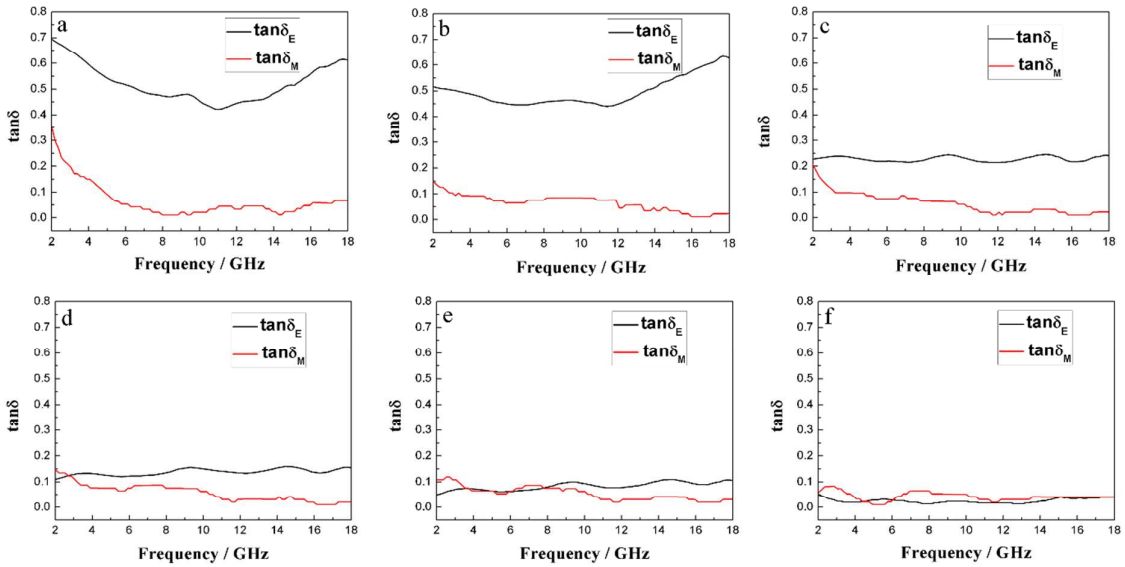

Fig.7. the loss tangent of dielectric and magnetic of (a) ox-SWCNHs, (b) S1, (c) S2, (d) S3, (e) S4 and (f) Fe_3O_4 NPs.

Conclusions

We have synthesized the Fe_3O_4/SWCNHs composites using a simple and effective approach and their microwave absorbing properties have been systematically studied. With a great impedance matching and a relatively large dielectric loss, the composite with 35.6wt.% exhibits a more excellent EM absorption performance than its counterparts. The maximum reflection loss of this composite with a thickness of 5.8mm is -38.84dB at 3.72GHz in S-band and the absorption bandwidths exceeding -10dB are 9.2GHz (from 3.2GHz to 12.4GHz) with the absorber thickness of 2-6mm. Besides, a second absorption peak appears when the absorber thickness is over 4mm and its maximum reflection loss can reach -10dB. Due to its easy accessibility and exceptional property, Fe_3O_4/SWCNHs may be used as attractive candidate for next-generation microwave absorption materials in the foreseeable future.

Acknowledgements

This work is supported by NSF of China (No. 21171013, No. 21471010, No. 21174017) and the Ministry of Science and Technology of China (No. 2013CB933402, No. 2011CB932601). The authors are also grateful to Prof. S. Gao at Peking University for providing magnetic property analysis of Fe_3O_4/SWCNHs composites.

Notes and references

1 A. Lerchl, *Asian J Androl,* 2013, **15**, 201.
2 (a) S. Tyagi, P. Verma, H.B. Baskey, R.C. Agarwala, V. Agarwala and T.C. Shami, *Ceram. Trans.,* 2012, **38**, 4561; (b) H. Hekmatara, M. Seifi and K. Forooraghi, *J. Magn. Magn. Mater.,* 2013, **346**, 186; (c) P. Bhattacharya, S. Sahoo and C. K. Das, *Eur. Polym. J.,* 2013, **7**, 212; (d) V.K. Singh, A. Shukla, M.K.Patra, L. Saini,R.K. Jani, S.R. Vadera and N. Kumar, *Carbon*, 2012, **50**, 2202; (e) P. Bhattacharya and C.K. Das, *J Mater Sci: Mater Electron,* 2013, **24**, 1927; (f) F. Nanni, P. Travaglia and M. Valentini, *Compos. Sci. Technol.,* 2009, **69**, 485.
3 (a) Y.W. Zhu, M. Shanthi, W.W. Cai, X.S. Li, J.W. Suk and Jeffrey R, *Adv. Mater.,* 2012, **22**, 3906; (b) G.J.H. Melvin, Q.Q. Ni and N. Toshiaki, *J. Alloys Compd.,* 2014, **615**, 84.
4 (a) J. Zheng, H.L. Lv, X.H. Lin, G.B. Ji, X.G. Li and Y.W. Du, *J. Alloys Compd.,* 2014, **589**, 174; (b) A.B. Zhang, M. Tang, X.F. Cao, Z.B. Lu and Y.T. Shen, *J Mater Sci.,* 2014, **49**, 4629.
5 (a) C. Wang, X.J. Han, P. Xu, X.L. Zhang, Y.C. Du and S.R. Hu, Appl. Phys. Lett., 2011, 98, 072906; (b) E.L. Ma, J.J. Li, N.Q.

Zhao, E.Z. Liu, C.N. He and C.S. Shi, *Mater Lett.,* 2013, **91**, 209; (c) S.W. Lu, W.K. Xu, X.H. Xiong, K.M. Ma and X.Q. Wang, J. Alloys Compd., 2014, **606**, 171; (d) Z.J. Wang, L.N. Wu, J.G. Zhou, W. Cai, B.Z. Shen and Z.H. Jiang, J. Phys. Chem. C, 2013, **117**, 5446.
6 Y. Liu, X.X. Liu and X.J. Wang. *Chin. Phys. B,* 2014, **23**, 117705.
7 G.J.H. Melvin, Q.Q. Ni, S. Yusuke and N. Toshiaki, *J Mater Sci.,* 2014, **49**, 5199.
8 Z.T. Zhu, X. Sun, G.X. Li, H.R. Xue, H. Guo and X.L. Fan, *J. Magn. Magn. Mater.,* 2015, **377**, 95.
9 S. Iijima, M. Yudasaka , R. Yamada, S. Bandow, K. Suenaga and F. Kokai, *Chem. Phys. Lett.,* 1999, **309**, 165.
10 S.Y. Zhu and G.B. Xu, Nanoscale, 2010, 2, 2538.
11 (a) N. Li, Z.Y. Wang, K.K. Zhao, Z.J. Shi, Z.N. Gu and S.K. Xu, *Carbon*, 2010, **48**, 1580; (b) M. Yudasaka, S. Iijima and V.H. Crespi, *Top. Appl. Phys.,* 2008, **111**, 605-629.
12 (a) H. Zheng, Y. Yang, M.G. Zhou and F.S. Li, Hyperfine Interact., 2009, **189**, 131; (b) F.S. Wen, F. Zhang and H. Zheng, *J. Magn. Magn. Mater.,* 2012, **324**, 2471; (c) Y.J. Liu, D. Song, C.X. Wu and J.S. Leng, *Composites Part B,* 2014, **63**, 34; (d) J. Kong, J.R. Liu, F.L. Wang, L.Q. Luan, M. Itoh and K. Machida, *Appl. Phys. A,* 2011, **105**, 351; (e) P.F. Guan, X.F. Zhang and J.J. Guo, *Appl. Phys. Lett.,* 2012, **101**, 153108; (f) C.L. Hou, T.H. Li, T.K. Zhao, H.G. Liu, L.H. Liu and W.J. Zhang, *New Carbon Mater.,* 2013, **28**, 184.
13 J.Q. Wan, W. Cai, X.X. Meng and E.Z. Liu, *Chem. Commun.,* 2007, **47**, 5004.
14 NA. Zubir, C. Yacou, J. Motuzas, X. Zhang and J.C. Diniz da Costa, *Sci. Rep.,* 2014, **4**, 4594.